

Holocene climate, dynamic landscapes and environmentally driven changes in human living conditions in Beijing



Gan Xie^{a,e,1}, Yi-Feng Yao^{a,1}, Jin-Feng Li^a, Jian Yang^a, Jia-De Bai^b, David K. Ferguson^c, Anjali Trivedi^{a,d}, Cheng-Sen Li^{a,**}, Yu-Fei Wang^{a,e,*}

^a State Key Laboratory of Systematic and Evolutionary Botany, Institute of Botany, Chinese Academy of Sciences, 20 Nanxincun, Xiangshan, Beijing 100093, China

^b Beijing Milu Ecological Research Center, Beijing 100076, China

^c University of Vienna, Department of Palaeontology, Althanstrasse 14, Vienna A-1090, Austria

^d Birbal Sahni Institute of Palaeosciences, 53 University Road, Lucknow, Uttar Pradesh 226007, India

^e University of Chinese Academy of Sciences, Beijing 100049, China

ARTICLE INFO

Keywords:

Beijing
Climatic change
East Asian monsoon region
Holocene
Human living environments
North China

ABSTRACT

The Holocene (11,500 cal a B.P. to the present) is marked by the beginning of the Neolithic Age and the origin of agriculture. Holocene climatic changes have certainly influenced vegetation successions and human living conditions. However, few studies have attempted to link the palaeo-ecological data with archaeological evidence to understand Holocene human-environmental interactions. Beijing, an early human settlement and the ancient and modern capital of China, is a hotspot for studying human activities and the development of civilization in Eastern Asia. The extensive literature on Holocene vegetation and climatic changes and the uninterrupted archaeological records from this region provide an excellent opportunity to explore how the climatic changes influenced the successions of vegetation and human living conditions since 12,000 cal a B.P. Here, we use Beijing as a case study and quantitatively reconstruct the Holocene climatic changes and the dynamic landscapes and human living conditions on the Beijing Plain based on compiled pollen data and archaeological literature. The results show that the mean annual temperature curve for Beijing during the early Holocene was similar to that of 90–30°N and has been the opposite since the middle to late Holocene. The mean annual precipitation curve is consistent with those from other monsoon regions in the Northern Hemisphere. The rising mean maximum monthly precipitation since 3330 cal a B.P. indicates the presence of more frequent rainstorms in summer, which suggests that the Beijing city government should prepare for more frequent heavy rainfalls and related geological disasters. In addition, the records from archaeological sites in Beijing show that human settlements first occurred in montane regions during the early Holocene before spreading into the plains during the middle Holocene. The warmer and wetter climate being suitable for farming probably drove this human migration. This study is an example of how to use past climatic data to understand current weather and the potential changes to human living environments that may occur under the current global warming trend.

1. Introduction

Beijing is famous for its early human settlements and its splendid history of oriental civilization. There is undisputed evidence of continuous prehistoric human activities in this region since, at least, the late Pleistocene; such sites include the Peking Man site, a formidable Palaeolithic human settlement from 780 to 400 ka (Shen et al., 2009), and the Caveman site from the late Palaeolithic Age, approximately

18 ka. The Holocene not only represents the beginning of the Neolithic Age and the advent of agriculture but is also a critical period in the formation and development of human society. Other Holocene archaeological sites found in Beijing, such as Donghulinren and Zhuan-nian from the early Holocene and Xueshan, Zhenjiangying, Shangzhai and Beiniantou from the middle to late Holocene, show a prosperous human society. Beijing became the capital for five Chinese dynasties (Liao, Jin, Yuan, Ming, Qing) after it had been established as the capital

* Correspondence to: Yu-Fei Wang, State Key Laboratory of Systematic and Evolutionary Botany, Institute of Botany, Chinese Academy of Sciences, 20 Nanxincun, Xiangshan, Beijing 100093, China.

** Corresponding author.

E-mail addresses: lics@ibcas.ac.cn (C.-S. Li), wangyf@ibcas.ac.cn (Y.-F. Wang).

¹ These authors contributed equally to this work.

of the Yan state in the Zhou Dynasty at approximately 3.0 ka B.P. and has an extensive historical and cultural heritage (see Su, 2000). Today, Beijing is still the political, economic and cultural centre of China.

On the other hand, numerous papers about Holocene vegetation and climatic changes of the Beijing area are available. After investigating the landforms and the distribution of fluvial sediments in Beijing, Shan et al. (1994) speculated that the climate was warm and wet in the mid-Holocene but became cold and dry in the late Holocene. In addition, there is evidence that extensive floods occurred frequently between 8.0 and 3.0 ka B.P. The ages of flooding events mentioned above were estimated by conventional radiocarbon dating (Yuan et al., 2002; Yao, 1991). For example, Yuan et al. (2002) found sediments in the Beijing Plain formed mainly of levee and crevasse splay deposits that had a maximum accumulation rate between 8.0 and 4.0 ka B.P., suggesting frequent occurrence of flooding during this time interval. After reviewing records of Holocene strata from the Yongding River Valley, Yao (1991) indicated that the erosional surface and silt layers formed by flooding occurred extensively in strata during 7.7–7.5 ka B.P., 5.2–4.6 ka B.P. and 3.2–3.0 ka B.P., corresponding to large-scale flooding events in the Beijing Plain during these periods. Based on original palynological research, both Yan et al. (1981) and Kong et al. (1982) inferred that the vegetation of Beijing was a grassland and/or coniferous forest from ca. 10.0–8.0 ka B.P., before becoming a broad-leaved forest or needle- and broad-leaved mixed forest ca. 8.0–2.0 ka B.P. and a grassland and/or coniferous forest since 2.0 ka B.P. They (Kong et al., 1982; Yan et al., 1981) suggested that Holocene temperature changes in Beijing were cold-warm-cold stages based on the relative abundance (RA) of conifer pollen, which displayed high-low-high values. Besides, some researchers have regarded the cereal pollen (Zhou, 2007) and starch grains (Yang et al., 2009) of *Vigna*, *Panicum miliaceum* and *Setaria italica* found on grinding stone tools at the Shangzhai site dating to 7.0–6.0 ka B.P. as a sign of the inception of agriculture in Beijing and have suggested (Zhou, 2007) that the climate was warm in this period, as reflected by the appearance of *Alnus*, *Carpinus*, *Tilia*, *Ulmus* etc. pollen, which stimulated the emergence of agriculture and the development of the Shangzhai civilization.

The literature on Holocene vegetation and climatic changes mentioned above and the uninterrupted archaeological records from Beijing provide an excellent opportunity to explore how climatic changes have influenced the successions of vegetation and human living conditions since 12,000 cal a B.P. Only a few current studies have linked the palaeo-ecological data to archaeological evidence to understand human-environmental interactions (Githumbi et al., 2017). Based on soil organic carbon isotopic evidence and archaeological literature from Kenya, Ambrose and Sikes (1991) found that hunter-gatherers preferred to live in forest-savanna ecotonal regions. Regional aridity during the mid-Holocene caused these ecotonal regions in the Central Rift Valley to recede to higher elevations, which probably led to a migration of hunter-gatherers. However, by combining palynological and archaeological data, Githumbi et al. (2017) have shown that although Kenya was dry at ~5000 cal a B.P., permanent water at Amboseli attracted abundant animals and facilitated human subsistence. Most other publications tend to treat human society and nature as distinct disciplines, with archaeologists focusing on the development of civilizations, while palaeo-ecologists tend to concentrate on Holocene vegetation and climatic changes. At the same time, the lack of quantitative climatic data prevents us from understanding the extent of climatic changes and their ecological impacts on vegetation and human society during the Holocene.

In this study, we use Beijing as a case study and quantitatively reconstruct the changes of climate of the Beijing Plain using the Coexistence Approach (CoA) (Mosbrugger and Utescher, 1997) based on formerly published palynological data, describe the dynamic landscapes and human habitats driven by these climatic changes using

compiled pollen data and archaeological literature, and explore the similarities and differences in the Holocene climate of Beijing and other regions worldwide.

2. Materials and methods

Beijing, 39°26′–41°03′ N, 115°25′–117°30′ E, is located in the East Asian Monsoon region of the North Temperate Zone. The land of Beijing slopes from the northwest to the southeast, with the Western Mountains in the west, the Yan Mountain in the north, and the plain to the south and east. Holocene pollen data from Beijing were available from nine sites with age controls from radiocarbon data, e.g., Zhou (2007) and Xie et al. (2016). Among these are four sites (Supplementary Fig. S1, sites 1–4 online) located in the lower montane regions of the Western Mountains and other sites located in the plain (Supplementary Fig. S1, sites 5–9 online). Sites in the lower montane regions (ca. 400–500 m above sea level (a.s.l.)) do not reflect the typical characteristics of the Western Mountains (reaching ca. 2300 m a.s.l.) with regard to the vertical vegetation zonation (Zhu, 1997) and climate. Therefore, we used pollen data from the Beijing Plain sites (ca. 40–100 m a.s.l.), rather than those from the lower montane regions, to reconstruct climatic changes and the dynamic landscapes of the Beijing Plain.

Here, we calibrated the radiocarbon dates from five sites on the Beijing Plain using <http://www.calpal-online.de> and divided the Holocene epoch into four time intervals: 11,899–10,597 cal a B.P., 7443–6863 cal a B.P., 5493–3334 cal a B.P. and 3334 cal a B.P. to present. Radiocarbon dates were rounded to the nearest 10 years (Foster et al., 2008), i.e., 11,900–10,600 (median: 11,250, hereafter) cal a B.P., 7440–6860 (7150) cal a B.P., 5490–3330 (4410) cal a B.P. and 3330 cal a B.P. to present (1670), and the median radiocarbon age of each range was used to represent these time intervals. For the process of dividing time intervals, see online Supplementary Fig. S2; for the original pollen data from the five sites on the Beijing Plain, see online Supplementary Table S1; and for the compiled pollen data, see online Supplementary Table S2.

In this article, we applied CoA (Mosbrugger and Utescher, 1997) to quantitatively reconstruct the Holocene climate of the Beijing Plain. Six climatic parameters were obtained: the mean annual temperature (MAT), the mean warmest monthly temperature (MWMT), the mean coldest monthly temperature (MCMT), the mean annual precipitation (MAP), the mean maximum monthly precipitation (MMap), and the mean minimum monthly precipitation (MMiP). The precipitation data were rounded to the nearest 1 mm.

The detailed steps used to calibrate the climatic interval of each parameter and the coexistence interval are explained below. First, we obtained plant taxa from the Holocene Beijing Plain based on the list of pollen taxa (see Supplementary Table S1, S2 online) and determined the distribution of these plant taxa following Wu and Ding (1999). Then, we compiled the modern climatic data within the distribution areas of each plant taxa were present using the *Surface Meteorological Data of China (1951–1980)* (IDBMC, 1983). Next, we calibrated the range of climatic parameters of each taxon by superimposing the climatic data of all of its locations. Finally, we calculated the coincidence intervals of the climatic parameters of all taxa from the same period, i.e., the Coexistence Intervals.

The palaeoclimatic fluctuations were depicted by the curves of the median values of the six climatic parameters calculated for each time interval. Here, we calculated the arithmetic mean of the upper and lower boundaries of the Coexistence Intervals, which was used to obtain the median value of each climatic parameter.

3. Results

The Holocene pollen assemblages of the Beijing Plain contained 81

palynomorphs (Supplementary Table S2 online), assigned to 56 families and 62 genera (note: some palynomorphs were identified at the family level in the related references), including angiosperms (43 families 43 genera), gymnosperms (three families seven genera), pteridophytes (five families four genera), and algae (five families eight genera). The Holocene pollen data of the four time intervals (Zones I–IV) are presented in Supplementary Table S2.

The six climatic parameters estimated by CoA based on pollen data from Zones I–IV (see Supplementary Figs. S3–S6 online) are listed in online Supplementary Table S3. The variations in temperature and precipitation (see Supplementary Fig. S7 online) are presented below.

3.1. MAT

The MAT increased from Zone I (0.4 to 14.9 °C, median: 7.7, delimited by *Ephedra* and *Abies*) to Zone II (3.5 to 18.6 °C, median: 11.1, restricted by *Corylus* and *Carpinus*), declined in Zone III (4.4 to 14.9 °C, median: 9.7, demarcated by *Ephedra* and *Castanea*), and then increased in Zone IV (10.2 to 13 °C, median: 11.6, delineated by *Swida* and *Cedrus*).

3.2. MWMT

The MWMT increased from Zone I (20.5 to 27.5 °C, median: 24, defined by *Betula* and *Abies*) to Zone II (22 to 27.5 °C, median: 24.8, restricted by *Betula* and *Carpinus*), rising in Zone III (22.9 to 27.5 °C, median: 25.2, demarcated by *Betula* and *Castanea*), and then remaining stable in Zone IV.

3.3. MCMT

The MCMT rose from Zone I (−23.9 to 5.9 °C, median: −9, delimited by *Ephedra* and *Abies*) to Zone II (−18.5 to 12.1 °C, median: −3.2, delimited by *Corylus* and *Carpinus*), declined in Zone III (−15.4 to 5.9 °C, median: −4.8, delimited by *Ephedra* and *Rhus*), and then increased in Zone IV (−5.6 to 2.4 °C, median: −1.6, demarcated by *Nitraria* and *Cedrus*).

3.4. MAP

The MAP increased from Zone I (304 to 1255 mm, median: 779, restricted by *Myriophyllum*) to Zone II (475 to 1484 mm, median: 980, delineated by *Carpinus* and *Corylus*), declined in Zone III (539 to 1255 mm, median: 897, defined by *Myriophyllum* and *Castanea*), and further decreased in Zone IV (539 to 1076 mm, median: 808, delimited by *Nitraria* and *Castanea*).

3.5. MMAP

The MMAP increased from Zone I (72 to 206 mm, median: 139, demarcated by *Ephedra* and *Myriophyllum*) to Zone II (104 to 246 mm, median: 175, bounded by *Typha* and *Alnus*), decreased slightly in Zone III (137 to 206 mm, median: 171, restricted by *Ephedra* and *Castanea*), and then remained stable in Zone IV.

3.6. MMiP

The MMiP decreased from Zone I (7 to 20 mm, median: 14, delimited by *Abies* and *Betula*) to Zone II (9 to 16 mm, median: 13, defined by *Ulmus* and *Humulus*), rose in Zone III (13 to 16 mm, median: 15, delimited by *Ulmus* and *Juglans*), and then remained stable in Zone IV.

4. Discussion

4.1. Holocene climatic changes of the Beijing Plain

The Holocene climate of the Beijing Plain can be evaluated using the MAT and MAP. The MAT increased from the beginning of the Holocene to 7150 cal a B.P., decreased to 4410 cal a B.P., and then increased until the present. Alternatively, the MAP rose from the earliest Holocene, reached its peak at 7150 cal a B.P., and then declined to the present-day level (see Supplementary Fig. S7 and Table S3 online).

Current meteorological data from the Beijing Plain are: MAT = 11.5 °C, MWMT = 25.8 °C, MCMT = −4.6 °C, MAP = 644.2 mm, MMAP = 212.3 mm, MMiP = 2.6 mm, based on the average values from 1951 to 1980 A.D. (IDBMC, 1983). Compared with the present data (see Supplementary Table S3 online), in 11,900–10,600 cal a B.P., the MAT was 4 °C lower, and the MAP was 140 mm higher; in 7440–6860 cal a B.P., the MAT was similar, while the MAP was 340 mm higher; in 5490–3330 cal a B.P., the MAT was 2 °C lower, while the MAP was 250 mm higher; and in 3330 cal a B.P. to present, the MAT was comparable, while the MAP was 160 mm higher.

In the Holocene, the MMAP of the Beijing Plain increased, but the MAP and MMiP decreased (see Supplementary Fig. S7 online). Since 3330 cal a B.P., the MMAP rose from 170 mm to its current 210 mm, while the MAP declined from 810 mm to 640 mm and MMiP from 15 mm to 3 mm (see Supplementary Table S3 online), which indicate an increasing seasonal difference in precipitation and more rainstorms in the summer. The rising MMAP since 3300 cal a B.P. seems to be coupled to the increasing frequency of fatal debris flows and landslides that have occurred in the past 150 years, as recorded by historical data from Beijing (Wu, 2001). This finding suggests that the Beijing city government should prepare for frequent heavy rainfalls in summer and related geological disasters.

4.2. Comparisons of the Holocene climatic changes between Beijing and other regions worldwide

4.2.1. Temperature

In general, the Holocene global temperature became warmer after the last ice age, then entered the warmest period during the last deglacial, the so-called Holocene Megathermal (Hafsten, 1970). Marcott et al. (2013) synthesized three zonal (90–30°N, 90–30°S and 30°N–30°S) mean temperature curves for the Holocene. In the zone of 90–30°N (Marcott et al., 2013), the temperature increased during 12,000–7000 cal a B.P., remained warm during 9500–5500 cal a B.P., and then decreased from ca. 5000 cal a B.P. until 1900 A.D. (Fig. 1b). A similar situation occurred on the Beijing Plain, i.e., the MAT increased during 11,250–7150 cal a B.P. (Fig. 1a) and a warm interval during 7440–6860 cal a B.P., corresponding to the Holocene Megathermal. Unlike other sites between 90 and 30°N (Marcott et al., 2013), the MAT of the Beijing Plain has increased since 4410 cal a B.P., a trend that has lasted to the present.

Line a, MAT of the Beijing Plain, this paper. Line b, zonal mean temperature anomaly curve reconstructed by records ranging from 90 to 30°N, redrawn from Marcott et al. (2013). Line c, MAT in Fanjing Mountain, Guizhou, redrawn from Qiao et al. (1996). Line d, MAT in Dai Lake, Inner Mongolia, redrawn from Xu et al. (2010).

Warming since the middle to late Holocene on the Beijing Plain was not an isolated phenomenon. In high latitude regions, the surface sea temperature (SST) of the subpolar North Atlantic increased from 7 ka B.P. (Rashid et al., 2016; Zhang et al., 2015), and this increase lasted until the present. The reduction in ice rafted debris (Bond and Bonani, 2001; Wanner et al., 2008) in the middle to high latitude North Atlantic indicates temperatures there have risen since ca. 5500 cal a B.P. In middle latitude regions, the SST (Wang, 2014) in the central

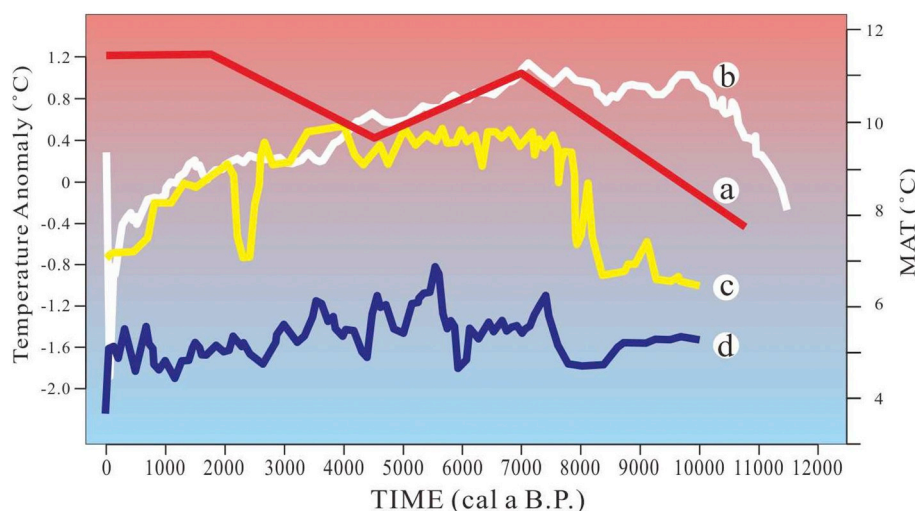


Fig. 1. Comparison between the MATs in China and the global temperature changes in the Holocene.

area of the South Yellow Sea (near Beijing) increased after 4 ka B.P. Moreover, the increasing $\delta^{18}\text{O}$ records from the Dundee Ice Cap (Shi et al., 1994) indicate an increased temperature since 5 ka B.P. At low latitudes, the SST began to increase after ca. 6000 cal a B.P. in the subtropical North Atlantic (deMenocal et al., 2000) and after 3–2 ka B.P. in the western tropical Pacific Ocean (Stott et al., 2004) (see Supplementary Fig. S8 online).

Nevertheless, the Holocene temperature changes were complex. Kim et al. (2004) found that the SST had mainly increased in the north Pacific and decreased in the north Atlantic since 7000 cal a B.P. Wanner et al. (2008) indicated that the SST in the Indo-Pacific area may have increased, decreased or showed no noteworthy changes since 6000 cal a B.P. The forcing factors remain unclear.

4.2.2. Precipitation

Wang and Ding (2008) identified six monsoon precipitation regions in intertropical continents: The South and North American Monsoon Region, the South and North African Monsoon Region, and the Asian and Australian Monsoon Region. We have compared the Holocene precipitation in the Beijing Plain to that of all six monsoon regions (Fig. 2).

Line a, MAP of the Beijing Plain, the East Asian Monsoon Region, this paper; Line b, regionally averaged moisture index curve for Northern China, the East Asian Monsoon Region, redrawn from Ran and Feng (2013); Line c, $^{87}\text{Sr}/^{86}\text{Sr}$ records from the Andaman Sea, the South Asian Monsoon Region, redrawn from Ali et al. (2015); Line d, Titanium ratios of sediments from the Ocean Drilling Program (ODP) Site 1002 in Venezuela, the North American Monsoon Region, redrawn from deMenocal et al. (2000); Line e, percentage terrigenous aeolian dust from ODP Site 658C in subtropical North Africa, the North African Monsoon Region, redrawn from Haug et al. (2001); Line f, a synthesized curve from two stalagmite $\delta^{18}\text{O}$ records in Indonesia, the Australian-Indonesian Monsoon Region, redrawn from Griffiths et al. (2009); Line g, the difference between $\delta^{18}\text{O}_{\text{calcite}}$ and $\delta^{18}\text{O}_{\text{ice}}$ records from two lake sediment cores in Peru, the South American Monsoon Region, redrawn from Seltzer et al. (2000); Line h, the $\delta^{15}\text{N}$ values from rock hyrax middens in Namibia, the South African Monsoon Region, redrawn from Chase et al. (2010); Line i, the summer insolation at 15°N and 15°S , redrawn from Chase et al. (2010). In addition, blue bars show the flooding events (Yao, 1991) in the Beijing Plain (Line a), and the bar widths represent the duration of time intervals. Here the radiocarbon dates were calibrated using <http://www.calpal-online.de>.

The Holocene precipitation trend from the Beijing Plain (Fig. 2a) was consistent with those of the Asian Monsoon Region (Fig. 2b, c) (Ali et al., 2015; Janelle et al., 2010; Ran and Feng, 2013), the North American Monsoon Region (Fig. 2d; Venezuela is in South America, but its latitude is ca. 10°N , and its precipitation is controlled by the North American Monsoon) (Haug et al., 2001), the North African Monsoon Region (Fig. 2e) (deMenocal et al., 2000) in the North Hemisphere and South African Monsoon Region (Fig. 2h) (Chase et al., 2010) in the South Hemisphere; the precipitation increased from 12,000 to 8000 cal a B.P., reached its peak ca. 9000–7000 cal a B.P., and then decreased to the present. However, in the Australian Monsoon Region (Fig. 2f) (Griffiths et al., 2009) and the South American Monsoon Region (Fig. 2g) (Seltzer et al., 2000) in the South Hemisphere, the precipitation decreased from the earliest Holocene to present.

Holocene precipitation trends in Northern/Southern Hemisphere monsoon regions are positively correlated with summer insolation at 15°N/S (Fig. 2i) (Chase et al., 2010), except for in the South African Monsoon Region in the South Hemisphere. Both the North and South African Monsoon Regions might primarily respond to summer insolation change in the Northern Hemisphere (Chase et al., 2010). Previous research (Braconnot et al., 2004; Cruz et al., 2005; Pokras and Mix, 1987) indicates that the precipitation in monsoon regions is controlled by summer insolation in the low latitude regions of the Northern/Southern Hemisphere. Increasing summer insolation in these low latitude regions probably raised their land temperatures and enhanced the land-sea temperature differences, increasing the intensity of summer monsoons and bringing more precipitation to monsoon domains (Wang, 2011).

The Holocene climate in Beijing, from $39^\circ26'41''\text{N}$, apparently was not only influenced by the amount of ice in high latitude regions (Kerr, 1987) but also by summer insolation at low latitudes. It is well-known that heat at the Earth's surface is derived from solar radiation. The surplus heat received in low latitude regions is transported to high latitudes to balance the energy regime (Ding, 2006). Monsoons are important for maintaining balance by transporting heat and moisture (Berger and André, 2009). Based on sediment analyses from the South China Sea, Wang et al. (1999) suggested that the intensity of the East Asian Summer Monsoon was strengthened during 17.0–10.7 ka B.P., which brought increased precipitation to South China and enhanced transport of heat from low to middle/high latitude regions. Here, we speculate that the East Asian Monsoon transported heat from low to high latitudes and influenced the climate in mid-latitude Beijing by heat balance during the Holocene. This transport was probably why the MAP

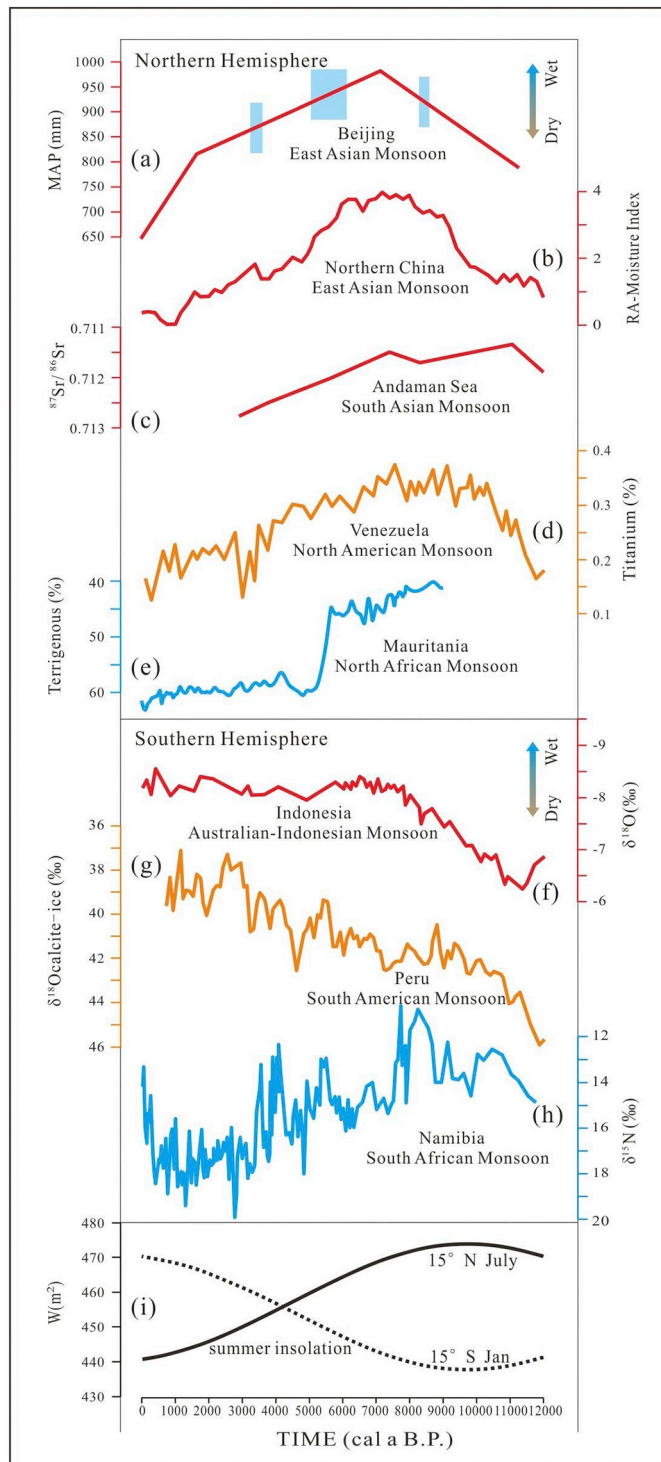


Fig. 2. Comparison of the MAP of Beijing and precipitation changes in different monsoon regions worldwide during the Holocene.

in the mid-latitude Beijing Plain (Fig. 2a) and the summer insolation at 15°N (Fig. 2i) consistently changed throughout the Holocene.

In both the east and west regions, there is evidence for a great prehistoric flood (Wang, 2011; Wu et al., 2016). High precipitation values between 7150 and 4410 cal a B.P. in the Beijing Plain may have resulted in a mid-Holocene flood (Wang, 2011; Wu et al., 2016). Abundant moisture during this period must have been transported to Beijing and to the eastern cradles of human civilization (Wu et al.,

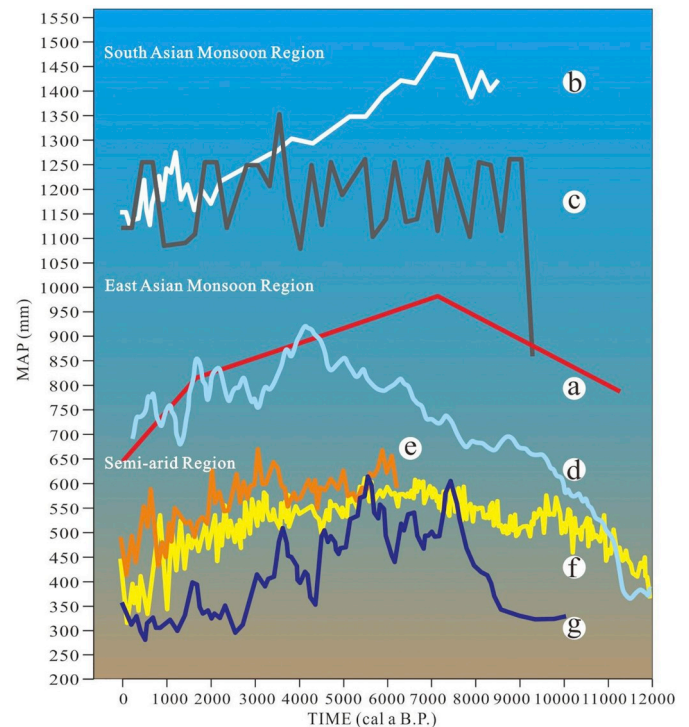


Fig. 3. Comparison between the Holocene MAP data from the Beijing Plain and other regions in China.

2016) by the East Asian Summer Monsoon.

4.3. Comparisons of the Holocene MAT and MAP data between Beijing and other regions in China

4.3.1. MAT

The MAT data from the Beijing Plain, the East Asian Monsoon Region, were higher than those from Fanjing Mountain, the South Asian Monsoon Region and Dai Lake, the Semi-arid Region during the same time interval in the Holocene: in 7440–6860 cal a B.P., the MAT of the Beijing Plain (39°26′–41°03′ N, ca. 40–100 m a.s.l.) (Fig. 1a), was 11.1 °C, which was 1–2 °C higher than that of Fanjing Mountain (27°48′–28°2′ N, ca. 2200 m a.s.l.) (Fig. 1c) (Qiao et al., 1996) and 5–6 °C higher than that of Dai Lake (40°29′–40°37′ N, ca. 1220 m a.s.l.) (Fig. 1d) (Xu et al., 2010). In 5490–3330 cal a B.P., the MAT of Beijing was 9.7 °C, which approximated that of Fanjing Mountain, while it was 3–5 °C higher than that of Dai Lake. Moreover, from 3330 cal a B.P. to present, the MAT of Beijing was 11.6 °C, which was 2–5 °C higher than that of Fanjing Mountain and 5–7 °C higher than that of Dai Lake. The higher altitude of Fanjing Mountain might be responsible for its lower MAT. If we compare the same altitude at Fanjing Mountain with the Beijing Plain (e.g., 100 m a.s.l., assuming a lapse rate of 6 °C/1000 m), the corrected MAT at Fanjing Mountain would be much higher than that of the Beijing Plain during the Holocene.

4.3.2. MAP

The Holocene MAP changes in the Beijing Plain (Fig. 3a) (East Asian Monsoon Region), Xingyun Lake (Fig. 3b) (Chen et al., 2014) and Hailu, Yunnan (Fig. 3c) (Song et al., 2012) (South Asian Monsoon Region) and Tianchi Lake, Gansu (Fig. 3e) (Zhao et al., 2010), Gong Lake, Shanxi (Fig. 3f) (Chen et al., 2015) and Dai Lake, Inner Mongolia (Fig. 3g) (Xu et al., 2010) (Semi-arid Region) were similar. This evidence might indicate that the precipitation patterns in the monsoonal and semi-arid regions of China developed in the Holocene.



Fig. 4. The early Holocene landscape of the Beijing Plain.

The MAP data since the earliest Holocene from the Beijing Plain (East Asian Monsoon Region) were 400–600 mm lower than those of Xingyun Lake and Haligu (South Asian Monsoon Region) and 200–400 mm higher than those of Dai Lake, Gong Lake and Tianchi Lake (Semi-arid Region) (Fig. 3). The MAP at Sihailongwan Maar Lake, Jilin, at the northern edge of the East Asian Monsoon Region (Fig. 3d), shifted from a Semi-arid Region level to an East Asian Monsoon Region level during the Holocene, which might have resulted from the strengthening and northwards expansion of the East Asian Monsoon (Stebich et al., 2015).

Line a, Beijing Plain, this paper. Line b, Xingyun Lake, Yunnan, redrawn from Chen et al. (2014). Line c, Haligu, Yunnan, redrawn from Song et al. (2012). Line d, Sihailongwan Maar Lake, Jilin, redrawn from Stebich et al. (2015). Line e, Tianchi Lake, Gansu, redrawn from Zhao et al. (2010). Line f, Gong Lake, Shanxi, redrawn from Chen et al. (2015). Line g, Dai Lake, Inner Mongolia, redrawn from Xu et al. (2010).

4.4. Dynamic landscapes of the Beijing Plain during the Holocene

By combining our reconstructed Holocene vegetation and climatic data from Beijing with archaeological literature (Su, 2000), we reconstructed the dynamic summer landscapes that existed near the Yongding River in the early (11,900–10,600 cal a B.P.), middle (7440–6860 cal a B.P.) and late (3330 cal a B.P. to present) stages of the Beijing Plain.

In the early Holocene, the climate of the Beijing Plain was cold and dry. Pollen data (Kong et al., 1982) show a mixed deciduous broad-leaved and coniferous forest vegetation type existed in the Beijing Plain during the early Holocene. These forests were dominated by *Betula* and *Pinus*, and grasslands were distributed in the Beijing Plain in mosaic patterns along the undulating terrain characterized by plain and hilly land, and were at different distances from rivers and lakes.

A mixed deciduous broad-leaved and coniferous forest flourished, with *Pinus*, *Betula*, *Tilia*, etc. dominating the plain (Fig. 4). Ferns such as Polypodiaceae and *Selaginella* grew under the trees and shrubs. *Ephedra*, *Artemisia*, Chenopodiaceae, *Polygonum*, *Thalictrum* and other herbs or shrubs formed a grassland/forest-grassland in a dry landscape far from water. Aquatic plants such as *Typha* lived in wetland, lakes and rivers,

while deer (Zhao, 2006) together with water birds, would have grazed on the Beijing Plain (Su, 2000).

A warm and wet climate prevailed on the Beijing Plain in the middle Holocene, i.e., during the Holocene Megathermal. An increasing number of broad-leaved trees such as *Acer*, *Celtis*, *Juglans*, *Quercus* and *Ulmus*, etc. enriched the forest. A deciduous broad-leaved forest probably replaced the mixed deciduous broad-leaved and coniferous forest on the plain (Fig. 5). Benefitting from the optimal climate, this forest would have prevailed throughout the plain. Polypodiaceae and Pteridaceae still grew in the understory of these forests. Aquatic plants such as *Myriophyllum* and *Typha* lived in water bodies or wetlands. Hygrophilous elements, such as *Alnus* and *Castanea*, grew near water. Abundant animal fossils reported from this period indicate a vital jungle world. Mammals such as roe deer (*Capreolus capreolus*), sika deer (*Cervus nippon*), and David's deer (Milu deer) (*Elaphurus davidianus*) roamed on the land. Concurrently, ancestors of poultry such as chicken (*Gallus* sp.) and duck (*Anas* sp.) were present. Burrowing animals such as zokor (*Myospalax psilurus*) dug holes underground, birds such as pigeons (*Columba* sp.) flew in the sky, and fishes such as catfish (*Parasilurus* sp.), goldfish (*Carassius auratus*), and snake-head (*Ophioccephalus* sp.) swam in the water (Su, 2000).

In the late Holocene, the MAP decreased, rivers and lakes retreated, and a warm and dry climate prevailed on the Beijing Plain (Fig. 6). A mixed deciduous broad-leaved and coniferous forest reappeared on the plain. During this time interval, the landscape was impacted not only by climatic changes but also by human activities, e.g., the establishment of Beijing City (Su, 2000). From then on, agricultural activities (Huang et al., 1996) reshaped the grassland/forest-grassland for farming. Flocks of sheep or goats grazed the land instead of deer.

4.5. Human migration from montane regions to the plain

The archaeological records indicate that human settlements first appeared in the montane regions during the early Holocene and occurred on the plain during the middle Holocene (Fig. 7). This discovery probably implies that the Holocene climatic changes impacted human survival and development.

Early Holocene sites are marked in red and middle Holocene sites are marked in yellow. 1, Zhuannian site, 9800 to 9200 a B.P. (Yu,



Fig. 5. The middle Holocene landscape of the Beijing Plain.



Fig. 6. The late Holocene landscape of the Beijing Plain.

2003); 2, Donghulin site, 11,170 to 9400 cal a B.P. (Hao et al., 2002; Xia et al., 2012); 3, Zhenjiangying site, 10,004 to 4234 cal a B.P. (Yu, 2007); 4, Xueshan site, 5590 to 3690 cal a B.P. (Han, 2003); 5, Beiniantou site, 7115 ± 120 cal a B.P. (Zhao et al., 1989); 6, Shangzhai site, 7443 ± 93 to 6863 ± 132 cal a B.P. (Zhou, 2007); the palace represents Beijing City at 1064 BCE (Su, 2000).

During the early Holocene, stone implements such as axes, scrapers and grinding stone tools, found in the mountains surrounding Beijing (Yu, 2003; Zhao, 2006), indicate the presence of small populations of hunter-gatherers. Compared with the open plain, the montane regions (Fig. 7, sites 1,2) seem to have provided better living conditions for human beings, with numerous caverns for shelters, more animals for hunting and nutritious plants for food during the cold and dry climate conditions.

During the middle Holocene, human settlements were found on the edges of the plain (Fig. 7, sites 4–6). Cereal pollen (Zhou, 2007) and starch grains (Yang et al., 2009) on grinding stone tools found in the plain indicate agricultural activities and higher productivity. The warmer and wetter climate that was suitable for farming made the Beijing Plain more attractive because it had abundant foodstuffs, which probably drove human beings to migrate from the hills into the plain.

During the late Holocene, Beijing City was established (1045 BCE) in the hinterland of the plain (Su, 2000) with gutters paved by cobblestones (Sheng, 2013), which probably indicated the ditch and/or irrigation system had been invented during that time, showing humans had an increasing capacity to deal with the more extreme climate and create better lives.

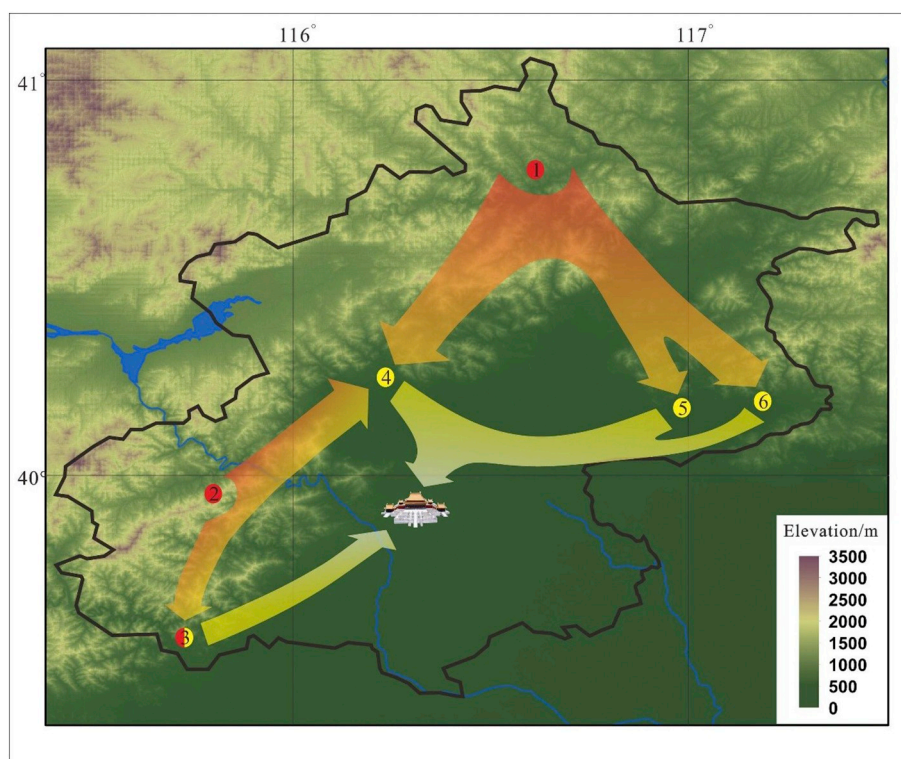


Fig. 7. Map showing Beijing Holocene human settlements and potential human migration routes.

Acknowledgements

The authors thank Ms. Ai-Li Li, at PE herbarium, Institute of Botany, Chinese Academy of Sciences, Beijing, China for drawing the Beijing Plain landscapes, and Dr. Jing-Xian Xu, Beijing Museum of Natural History, Beijing, China, Dr. Hao Hui, Beijing University of Technology, Beijing, China, and Prof. Ya-Meng Li, Linyi University, Shandong, China for providing references. This research was supported by the Project of Beijing Academy of Science and Technology (No. PXM201417821-8000005), China National Key Basic Research Program (No. 2014CB954201), the Strategic Priority Research Program of Chinese Academy of Sciences (No. XDB26000000), State Key Laboratory of Systematic and Evolutionary Botany (No. LSEB 2012-09), and the Chinese Academy of Sciences President's International Fellowship Initiative (Nos. 2016VBC063 and 2018VBA0016).

Authors' contributions

CSL, YFW and JDB conceived the ideas, GX, YFY, JFL and JY collected the literature, GX extracted and compiled the data, GX, YFY, JFL and JY made statistic analysis, GX, JFL and JY drew the figures and tables except landscapes, GX, YFW and AT wrote the first draft of this manuscript, DKF rewrote some of the discussion and corrected the final manuscript, while all authors contributed substantially to revisions.

Competing interests

We have no competing interests.

Appendix A. Supplementary data

Supplementary data to this article can be found online at <https://doi.org/10.1016/j.earscirev.2019.02.017>.

References

- Ali, S., Hathorne, E.C., Frank, M., Gebregiorgis, D., Stattegger, K., Stumpf, R., Kutterolf, S., Johnson, J.E., Giosan, L., 2015. South Asian monsoon history over the past 60 kyr recorded by radiogenic isotopes and clay mineral assemblages in the Andaman Sea. *Geochem. Geophys. Geosyst.* 16 (2), 505–521.
- Ambrose, S.H., Sikes, N.E., 1991. Soil carbon isotope evidence for holocene habitat change in the Kenya rift valley. *Science* 253 (5026), 1402.
- Berger, André, 2009. Monsoon and general circulation system. *Sci. Bull.* 54 (7), 1111–1112.
- Bond, G., Bonani, G., 2001. Persistent solar influence on North Atlantic climate during the Holocene. *Science* 294 (5549), 2130–2136.
- Braconnot, P., Harrison, S.P., Joussaume, S., Hewitt, C.D., Kitoh, A., Kutzbach, J.E., Liu, Z., Otto-Bliesner, B., Syktus, J., Weber, S., 2004. Evaluation of PMIP Coupled Ocean-Atmosphere Simulations of the Mid-Holocene, Past Climate Variability through Europe and Africa. Springer, pp. 515–533.
- Chase, B.M., Meadows, M.E., Carr, A.S., Reimer, P.J., 2010. Evidence for progressive Holocene aridification in southern Africa recorded in Namibian hyrax middens: implications for African Monsoon dynamics and the "African Humid Period". *Quat. Res.* 74 (1), 36–45.
- Chen, F., Chen, X., Chen, J., Zhou, A., Wu, D., Tang, L., Zhang, X., Huang, X., Yu, J., 2014. Holocene vegetation history, precipitation changes and Indian Summer Monsoon evolution documented from sediments of Xingyun Lake, south-West China. *J. Quat. Sci.* 29 (7), 661–674.
- Chen, F., Xu, Q., Chen, J., Birks, H.J.B., Liu, J., Zhang, S., Jin, L., An, C., Telford, R.J., Cao, X., 2015. East Asian summer monsoon precipitation variability since the last deglaciation. *Sci. Rep.* 5.
- Cruz, F.W., Burns, S.J., Karmann, I., Sharp, W.D., Vuille, M., Cardoso, A.O., Ferrari, J.A., Dias, P.L.S., Viana, O., 2005. Insolation-driven changes in atmospheric circulation over the past 116,000 years in subtropical Brazil. *Nature* 434 (7029), 63–66.
- Ding, Z., 2006. The Milankovitch Theory of Pleistocene glacial cycles: challenges and chances. *Quat. Sci.* 26 (5), 710–717.
- Foster, G.C., Chiverrell, R.C., Harvey, A.M., Dunsford, J.A., 2008. Catchment hydrogeomorphological responses to environmental change in the Southern Uplands of Scotland. *Holocene* 18 (6), 935.
- Githumbi, E.N., Kariuki, R., Shoemaker, A., Courtney-Mustaphi, C.J., Chuhilla, M., Richer, S., Lane, P., Marchant, R., 2017. Pollen, people and place: multidisciplinary perspectives on Ecosystem change at Amboseli, Kenya. *Front. Earth Sci.* 5 (113).
- Griffiths, M.L., Drysdale, R.N., Gagan, M., Zhao, J.-X., Ayliffe, L., Hellstrom, J.C., Hantoro, W., Frisia, S., Feng, Y.-X., Cartwright, I., 2009. Increasing Australian-Indonesian monsoon rainfall linked to early Holocene Sea-level rise. *Nat. Geosci.* 2 (9), 636–639.
- Hafsten, U., 1970. A sub-division of the Late Pleistocene Period on a synchronous basis, intended for global and universal usage. *Palaeogeogr. Palaeoclimatol. Palaeoecol.* 7 (4), 279–296.
- Han, J., 2003. The first stage culture of Xueshan site. *Huaxia Archaeol.* (4), 46–54.

- Hao, S., Ma, X., Xia, Z., Zhao, C., Yuan, S., Yu, J., 2002. The early Holocene loess section in the Donghulin Site near Zhaitang in Beijing. *Acta Geol. Sin.* 76 (3), 420–430.
- Haug, G.H., Hughen, K.A., Sigman, D.M., Peterson, L.C., Röhl, U., 2001. Southward migration of the intertropical convergence zone through the Holocene. *Science* 293 (5533), 1304–1308.
- Huang, C., Kong, Z., Pu, Q., Min, L., Ji, C., Shen, G., Pang, Q., Liu, C., Liu, Y., Zhai, X., 1996. Kunming Lake Sediments (over 3500 Years), Summer Palace. China Ocean Press, Beijing.
- IDBMC, 1983. Land climate data of China (1951–1980) (part I). China Meteorological Press.
- Janelle, S., Fernando, S., Jan, F., Domingo, M., Henk, H., 2010. Paoay Lake, northern Luzon, the Philippines: a record of Holocene environmental change. *Glob. Chang. Biol.* 16 (6), 1672–1688.
- Kerr, R.A., 1997. Milankovitch climate cycles through the ages. *Science* 235 (4792), 973–974.
- Kim, J.H., Rimbou, N., Lorenz, S.J., Lohmann, G., Nam, S.I., Schouten, S., Rühlemann, C., Schneider, R.R., 2004. North Pacific and North Atlantic sea-surface temperature variability during the Holocene. *Quat. Sci. Rev.* 23 (20), 2141–2154.
- Kong, Z., Du, N., Zhang, Z., 1982. Vegetational development and climatic changes in the last 10000 years in Beijing. *Acta Bot. Sin.* 2, 013.
- Marcott, S.A., Shakun, J.D., Clark, P.U., Mix, A.C., 2013. A reconstruction of regional and global temperature for the past 11,300 years. *Science* 339 (6124), 1198–1201.
- deMenocal, P., Ortiz, J.D., Guilderson, T., Adkins, J., Sarnthein, M., Baker, L., Yarusinsky, M., 2000. Abrupt onset and terminations of the African humid period: rapid climate responses to gradual insolation forcing. *Quat. Sci. Rev.* 19 (1), 347.
- Mosbrugger, V., Utescher, T., 1997. The coexistence approach—a method for quantitative reconstructions of Tertiary terrestrial palaeoclimate data using plant fossils. *Palaeogeogr. Palaeoclimatol. Palaeoecol.* 134 (1), 61–86.
- Pokras, E.M., Mix, A.C., 1987. Earth's precession cycle and Quaternary climatic change in tropical Africa. *Nature* 326 (6112), 486–487.
- Qiao, Y., Chen, P., Shen, C., Sun, Y., Zhou, Q., Jiang, M., 1996. Quantitative reconstruction of vegetation and climate of Fanjingshan section in Guizhou during last 10000 years. *Geochimica* 25 (5), 445–457.
- Ran, M., Feng, Z., 2013. Holocene moisture variations across China and driving mechanisms: a synthesis of climatic records. *Quat. Int.* 313, 179–193.
- Rashid, H., Marche, B., Vermooten, M., Parry, D., Webb, M., Brockway, B., Langer, K., 2016. Comment on “Asynchronous variation in the East Asian winter monsoon during the Holocene” by Xiaojian Zhang, Liya Jin, and Na Li. *J. Geophys. Res. Atmos.* 121 (4), 1611–1614.
- Seltzer, G., Rodbell, D., Burns, S., 2000. Isotopic evidence for late Quaternary climatic change in tropical South America. *Geology* 28 (1), 35–38.
- Shan, Q., Yang, H., Liu, L., 1994. The environment evolution of Quaternary of Beijing-Tongxian region. *Beijing Geol.* (4), 1–7.
- Shen, G., Gao, X., Gao, B., Granger, D.E., 2009. Age of Zhoukoudian *Homo erectus* determined with $^{26}\text{Al}/^{10}\text{Be}$ burial dating. *Nature* 458 (458), 198–200.
- Sheng, H., 2013. Archaeological discovery and research on the Xia, Shang and Zhou Dynasties in Fangshan District, Beijing. *J. Capital Normal Univ. (Social Sciences Edition)* 2, 27–34.
- Shi, Y., Kong, Z., Wang, S., Tang, L., Wang, F., Yao, T., Zhao, X., Zhang, P., Shi, S., 1994. The climatic fluctuation and important events of Holocene Megathermal in China. *Sci. China Ser. B* 37 (3), 353–365.
- Song, X., Yao, Y., Wortley, A., Paudyal, K., Yang, S., Li, C., Blackmore, S., 2012. Holocene vegetation and climate history at Haligu on the Jade Dragon snow mountain, Yunnan, SW China. *Clim. Chang.* 113 (3–4), 841–866.
- Stebich, M., Rehfeld, K., Schlütz, F., Tarasov, P.E., Liu, J., Mingram, J., 2015. Holocene vegetation and climate dynamics of NE China based on the pollen record from Sihailongwan Maar Lake. *Quat. Sci. Rev.* 124, 275–289.
- Stott, L., Cannariato, K., Thunell, R., Haug, G.H., Koutavas, A., Lund, S., 2004. Decline of surface temperature and salinity in the western tropical Pacific Ocean in the Holocene epoch. *Nature* 431 (7004), 56–59.
- Su, T., 2000. Intergration of Archaeological Researches in Beijing. vols. 2–4 Beijing Publishing House, Beijing.
- Wang, S., 2011. The Holocene Climate Change. China Meteorological Press, Beijing.
- Wang, L., 2014. Sediment Record of Paleoenvironment of the Central Mud of the South Yellow Sea and its Respose to the East Asian Monsoon during the Holocene. Ocean University of China.
- Wang, B., Ding, Q., 2008. Global monsoon: Dominant mode of annual variation in the tropics. *Dynamics of Atmospheres and Oceans* 44 (3), 165–183.
- Wang, L., Sarnthein, M., Grootes, P.M., Erlenkeuser, H., 1999. Millennial reoccurrence of century-scale abrupt events of East Asian Monsoon: a possible heat conveyor for the global deglaciation. *Paleoceanography* 14 (6), 725–731.
- Wanner, H., Beer, J., Bütikofer, J., Crowley, T.J., Cubasch, U., Flückiger, J., Goosse, H., Grosjean, M., Joos, F., Kaplan, J.O., 2008. Mid-to late Holocene climate change: an overview. *Quat. Sci. Rev.* 27 (19), 1791–1828.
- Wu, Z., 2001. The mud-rock flow disaster and their touch off condition by rainfall in Beijing area. *Res. Soil Water Conserv.* 8 (1), 67–72.
- Wu, Z., Ding, T., 1999. Seed Plants of China. Yunnan Science and Technology Press, Kunming, Yunnan (Electronic publication in Chinese).
- Wu, Q., Zhao, Z., Liu, L., Granger, D.E., Wang, H., Cohen, D.J., Wu, X., Ye, M., Baryosef, O., Lu, B., 2016. Outburst flood at 1920 BCE supports historicity of China's Great Flood and the Xia dynasty. *Science* 353 (6299), 579–582.
- Xia, Z., Zhang, J., Liu, J., Zhao, C., Wu, X., 2012. Analysis of the ecological environment around 10000 a BP in Zhaitang area, Beijing: a case study of the Donghulin Site. *Chin. Sci. Bull.* 57 (4), 360–369.
- Xie, G., Bai, J., Xu, J., Hao, H., Li, J., Yao, Y., Zhang, L., Li, C., Yang, J., Wang, Y., 2016. Research advances in the vegetation and climate of the Beijing Region, North China since the Holocene. *Bull. Bot.* 51 (6), 872–881.
- Xu, Q., Xiao, J., Li, Y., Tian, F., Nakagawa, T., 2010. Pollen-based quantitative reconstruction of Holocene climate changes in the Daihai Lake area, Inner Mongolia, China. *J. Clim.* 23 (11), 2856–2868.
- Yan, F., Ye, Y., Mai, X., Lie, Y., 1981. On the environment and geological age of two ores in Beijing region from sporo-pollen analysis. *Seismol. Geol.* 3 (1), 51–65.
- Yang, X., Yu, J., Lv, H., Cui, T., Diao, X., Kong, Z., Liu, C., Ge, Q., 2009. Starch grain analysis reveals function of grinding stone tools at Shangzhai site, Beijing. *Sci. China Ser. D Earth Sci.* (9), 1266–1273.
- Yao, L., 1991. The regularity of the flood of the Yongding River during the Holocene. *Geogr. Res.* 10, 59–67.
- Yu, D., 2003. The significances of Zhuannian site on agriculture archaeology. *Agric. Archaeol.* (3), 56–58.
- Yu, X., 2007. The Zhenjiangying culture. *Stor. Relics* (4), 3–9.
- Yuan, B., Deng, C., Lv, J., Jin, C., Wu, Y., 2002. A late Quaternary accumulation period and the Prehistoric Flood in Beijing plain. *Quat. Sci.* 22 (5), 474–482.
- Zhang, X., Jin, L., Li, N., 2015. Asynchronous variation in the East Asian winter monsoon during the Holocene. *J. Geophys. Res. Atmos.* 120 (11), 5357–5370.
- Zhao, C., 2006. The Donghulin site, in the Mentougou District of Beijing. *Archaeology* 7, 3–8.
- Zhao, F., Yu, J., Wang, W., Yuan, J., 1989. Survey and excavation in Beiniantou site, a neolithic site in Pinggu District, Beijing. *Cult. Relics* (8), 9–16.
- Zhao, Y., Chen, F., Zhou, A., Yu, Z., Zhang, K., 2010. Vegetation history, climate change and human activities over the last 6200 years on the Liupan Mountains in the southwestern Loess Plateau in Central China. *Palaeogeogr. Palaeoclimatol. Palaeoecol.* 293 (1), 197–205.
- Zhou, K., 2007. Environmental archaeological research in the Neolithic Shangzhai site, Beijing. *Cult. Relics Central China* 2, 19–24.
- Zhu, H., 1997. A discussion on the way of zonation of vegetation on the shade slope of Baihuashan mountain, Beijing. *J. Beijing For. Univ.* 19 (4), 59–63.